International Journal of Bioprinting

RESEARCH ARTICLE

3D bioprinting of ultrashort self-assembling peptides to engineer scaffolds with different matrix stiffness for chondrogenesis

Dana M. Alhattab[1,2,3], Zainab Khan[1,2,3], Salwa Alshehri[4], Hepi H. Susapto[1,5], Charlotte A. E. Hauser[1,2,3]*

[1]Laboratory for Nanomedicine, Bioengineering Program, Division of Biological & Environmental Science & Engineering (BESE), King Abdullah University of Science and Technology (KAUST), Thuwal, Saudi Arabia

[2]Computational Bioscience Research Center (CBRC), KAUST, Thuwal, Saudi Arabia

[3]Red Sea Research Center (RSRC), KAUST, Thuwal, Saudi Arabia

[4]Biochemistry Department, Faculty of Science, University of Jeddah, Jeddah 21577, Saudi Arabia

[5]Mechanobiology Institute, National University of Singapore, 117411, Singapore, Singapore

Abstract

Articular cartilage is a nonvascularized and poorly cellularized tissue with a low self-repair capacity. Therefore, damage to this tissue due to trauma or degenerative joint diseases such as osteoarthritis needs a high-end medical intervention. However, such interventions are costly, have limited healing capacity, and could impair patients' quality of life. In this regard, tissue engineering and three-dimensional (3D) bioprinting hold great potential. However, identifying suitable bioinks that are biocompatible, with the desired mechanical stiffness, and can be used under physiological conditions is still a challenge. In this study, we developed two tetrameric self-assembling ultrashort peptide bioinks that are chemically well-defined and can spontaneously form nanofibrous hydrogels under physiological conditions. The printability of the two ultrashort peptides was demonstrated; different shape constructs were printed with high shape fidelity and stability. Furthermore, the developed ultrashort peptide bioinks gave rise to constructs with different mechanical properties that could be used to guide stem cell differentiation toward specific lineages. Both ultrashort peptide bioinks demonstrated high biocompatibility and supported the chondrogenic differentiation of human mesenchymal stem cells. Additionally, the gene expression analysis of differentiated stem cells with the ultrashort peptide bioinks revealed articular cartilage extracellular matrix formation preference. Based on the different mechanical stiffness of the two ultrashort peptide bioinks, they can be used to fabricate cartilage tissue with different cartilaginous zones, including the articular and calcified cartilage zones, which are essential for engineered tissue integration.

Keywords: Ultrashort self-assembling peptide; 3D bioprinting; Peptide bioink; Chondrogenic differentiation

***Corresponding author:**
Charlotte A. E. Hauser
(charlotte.hauser@kaust.edu.sa)

Citation: Alhattab DM, Khan Z, Alshehri S, *et al*., 2023, 3D bioprinting of ultrashort self-assembling peptides to engineer scaffolds with different matrix stiffness for chondrogenesis. *Int J Bioprint*.
https://doi.org/10.18063/ijb.719

Received: February 12, 2023
Accepted: February 26, 2023
Published Online: March 24, 2023

1. Introduction

Hydrogels are a class of materials composed of hydrophilic networks of crosslinked polymers, which can be used to mimic the extracellular matrix (ECM) of the body[1]. These materials have been used in tissue engineering for various applications, including chondrogenic engineering. They can create a three-dimensional (3D) structure to support the growth of cells and can be used to deliver drugs and other therapeutic agents[2]. A variety of natural and synthetic hydrogels, including collagen, polyacrylamide, and hyaluronic acid-based hydrogels, have been used in chondrogenic engineering. However, one of the main disadvantages of natural hydrogels, such as collagen and hyaluronic acid, is their limited mechanical strength, which can limit their use in specific applications[3]. Moreover, the synthetic polyacrylamide hydrogel are poorly biocompatible, very costly, and difficult to work with[4,5].

On the other hand, ultrashort peptide hydrogels have gained recognition recently, particularly for biomedical applications and tissue engineering[6]. These ultrashort peptide hydrogels possess a range of properties that make them particularly attractive for tissue engineering and regenerative medicine applications. For example, they are biocompatible, biodegradable, and nontoxic, and have the spontaneous ability to rapidly form a hydrogel at concentrations as low as 0.01% under physiological conditions[6]. Furthermore, these ultrashort peptide hydrogels can be designed to have a range of mechanical properties, such as stiffness, elasticity, and strength, making them highly suitable for use in various tissue engineering applications[6].

Chondrogenic engineering is a rapidly growing field of biotechnology that focuses on using stem cells and other cell types to create new tissues and organs[7]. It is a complex and challenging field of research since it requires the development of effective and safe methods for delivering therapeutic agents to the target tissue, controlling the growth and differentiation of the engineered cells, and ensuring that the engineered cells can integrate into the existing tissue and function properly[8]. Recent studies have demonstrated that 3D bioprinting may be a promising *in situ* cartilage regeneration strategy[9-12]. 3D bioprinting has provided an avenue for the regeneration of functional cartilage in many applications[13].

3D bioprinting techniques are mainly divided into three main categories: material extrusion, material jetting, and vat polymerization[14]. The most widely used technique is extrusion-based printing, involving the extrusion of biomaterials from nozzles using either mechanical or pressure-based pumping systems. The extrusion is conducted layer-by-layer with the nozzle suspended above the print and carried along a set platform. This approach allows the extrusion of bioinks with high cell density, which makes them preferred candidates for cellular 3D bioprinting. It is also cost-effective and easily customizable. However, its main tradeoff is its limitations in resolution and speed[15].

Another procedure is material jetting, which uses an inkjet technique for 3D-bioprinting desired objects. It involves droplet formation through piezo-electric or thermally induced bubbles and downstream ejection created by a volumetric change upstream of the nozzle[16-20]. Its high printing speeds, cost-effectiveness, and contactless method that reduces contamination risks make it a viable 3D bioprinting approach. However, the fact that it is more suitable for highly viscous bioinks makes it less possible for cellular 3D bioprinting[15]. Hence, extrusion-based approaches are preferred for the creation of cell-laden bioprinted structures.

The final technique for 3D bioprinting is vat photopolymerization. It includes several approaches, such as stereolithography (SLA) and digital light processing (DLP)[14]. The primary approach comprises solidifying a photo-initiated liquid material using a laser or LCD light source. A platform upon which the liquid is set, is continuously raised after the light source hardens each layer, thus creating a high-resolution print structure[21]. In SLA, the laser is directed at specific solidification points to form layers. On the other hand, in DLP, the laser is directed at the entire surface, and the use of a mask between it and the liquid achieves solidification of the desired regions. Intuitively, this approach offers very high resolution but does not allow the incorporation of cells during the 3D bioprinting process, making it challenging to incorporate high cell densities into a construct[21].

Different 3D bioprinting materials have been used to fabricate cartilage constructs. Xue *et al.* tested the possibility of culturing cartilage precursor cells with poly(3-hydroxybutyrate-co-3-hydroxyvalerate) (PHBV) to manufacture tissue-engineered cartilage[22]. Another group reported the creation of cartilage constructs using collagen hydrogels and human mesenchymal stromal cells (MSCs)[23]. However, one of the main disadvantages of PHBV is its relatively high cost. Additionally, the production process for PHBV is more complex and energy-intensive than other thermoplastics, further increasing the cost[24]. On the other hand, collagen is a protein that is sensitive to temperature and pH changes, which can cause it to degrade over time. This could result in a reduction of the structural integrity of the printed construct, making it difficult to maintain its shape and form. Additionally, collagen is

prone to denaturation, which can lead to a decrease in its biocompatibility and cell viability[25].

The field of 3D bioprinting has advanced rapidly in recent years, with many promising applications in biomedical engineering, regenerative medicine, and tissue engineering[26]. To further progress the field, researchers have explored various methods for optimizing 3D bioprinting processes. One such method is the use of ultrashort peptide bioinks[26]. Our previous study demonstrated the potential of such bioinks for optimizing a 3D bioprinting process, and using these bioinks results in improved printability, enhanced mechanical properties, and biocompatibility[26]. Furthermore, using ultrashort peptide bioinks in 3D bioprinting can result in a more cost-effective process. Overall, 3D bioprinting for chondrogenic applications is an exciting and rapidly advancing field of research[27]. It has the potential to revolutionize the way we treat cartilage-related diseases and injuries and could provide a more precise and efficient way to create tissue-engineered cartilage[28].

In this study, we aimed to investigate at the molecular level the potential of using two tetrameric ultrashort peptide bioink in cartilage tissue engineering. We analyzed the printability of both ultrashort peptides at physiological conditions, studied their biocompatibility, and demonstrated their ability to induce chondrogenic differentiation of human bone marrow mesenchymal stem cells (hBM-MSCs), which are ultimately to be used in cartilage tissue engineering.

2. Materials and methods

2.1. Design and synthesis of self-assembling ultrashort peptides

Two peptide sequences were used in this study: Ac-Ile-Ile-Cha-Lys-NH2 (IIZK) and Ac-Ile-Cha-Cha-Lys-NH2 (IZZK). Both ultrashort peptides (IIZK and IZZK) were synthesized by solid-phase peptide synthesis (SPPS) using CS136X CS Biopeptide synthesizer. The peptide coupling was conducted on rink amide resin using a mixture of TBTU (3eq.), HOBt (3eq.), DIPEA (6 eq.), and Fmoc-protected amino acid (3eq.). Piperidine/DMF at 20% (v/v) was used to deprotect the Fmoc group on the N-terminus of the ultrashort peptide sequence and proceed to the next coupling step. After coupling the last amino acid to the peptide sequence, the sequence was capped with an acetyl group. The peptide was then cleaved from the resin with an acidic solution of trifluoroacetic acid (TFA), triisopropylsilane (TIS), and water for 2 h. The peptide was subsequently collected, and cold diethyl ether was added to induce peptide precipitation that was kept standing overnight at 4°C. The precipitated peptide was separated from the supernatant by centrifugation and kept in a vacuum desiccator for drying. The collected peptide was purified using Agilent 1260 Infinity Prep-HPLC with Zorbax PrepHT SB-C18 column for 12 min at 20 mL/min flow rate. MilliQ water and acetonitrile containing 0.1% formic acid were used as mobile phases. The purified peptide was collected with more than 60% in yield.

2.2. Characterization of ultrashort peptide hydrogel

2.2.1. Peptide gelation and hydrogel formation

Peptide gelation and hydrogel formation potential for IIZK and IZZK peptides were evaluated as previously described[29]. Briefly, the peptide powder was dissolved in 0.9 mL of MilliQ water and vortexed until a clear and homogeneous solution was observed. Then 0.1 mL of 10× phosphate-buffered saline (PBS; without Ca^{2+} and Mg^{2+}) was added to the peptide solution. The vial was kept undisturbed, and the soft solid hydrogel formation was observed using the vial inversion method. The time and minimum concentration at which each peptide did form a hydrogel were identified.

2.2.2. Scanning electron microscopy

Scanning electron microscopy (SEM) was used to identify the nanofibrous topography of peptide hydrogel at different peptide concentrations. First, samples for SEM imaging were prepared by dehydrating peptide hydrogels in a gradually increasing ethanol concentration. Then, the dehydrated gel was transferred and dried in a Tousimis Automegasamdri-916B series C Critical Point Dryer. The dried sample was sputter-coated with 5-nm Ir thickness before imaging. SEM images were taken using an FEI Magellan XHR Scanning Electron Microscope with an accelerating voltage of 3 kV.

2.2.3. Rheology measurements of ultrashort peptide hydrogels

Mechanical stiffness of IIZK and IZZK peptides was analyzed using a TA Ares-G2 Rheometer equipped with an advanced Peltier system (APS). The mechanical stiffness of the peptide gels was measured at ambient temperature using an 8-mm parallel plate with a gap of 1.8 mm, between the upper and lower plates. The hydrogel samples were made by mixing 13 mg/mL peptide solution with 7× PBS with a ratio of two to one based on the flow rate ratio from Pump 1 against Pump 2+3. These gels were prepared 1 day before measurement using the ring-cast method. For each peptide, six replicates were prepared to control the accuracy of the measurements. The stiffness was analyzed through two successive tests: frequency sweep and amplitude sweep. First, the frequency sweep was performed for a range of angular frequency of 0.1–100 rad/s with a strain of 0.1%. Then, the amplitude sweep was performed by applying a

gradual increase of strain from 0.01% to 100% at 1 rad/s angular frequency.

2.3. 3D bioprinting

2.3.1. 3D bioprinter setup and printing parameters optimization

An in-house developed robotic 3D bioprinter was used for the 3D bioprinting experiments[30]. The printer components included a five-degree-of-freedom robotic arm, a custom-designed coaxial nozzle, a set of microfluidic pumps, and a heated bed. The robotic arm was interfaced with Repetier-Host to slice files into gcode for 3D printing, and printing files were designed in SolidWorks®. The coaxial nozzle was fabricated to house three inlets and a single outlet, with a final inner diameter of 0.5 mm. The three inlets included a channel for the peptide, another one for the cells, and the third inlet for PBS concentration >1× to fasten the gelation process of the peptide. The commercial microfluidic pumps were controlled simultaneously during printing through a Labview-based graphical user interface.

The printing parameters used were as described before[29]; the peptide concentration was set to 13 mg/mL for the two ultrashort peptides, a concentration of 7× PBS was used for the gelation of both ultrashort peptides, and the heatbed was set to 37°C. The pump flow rates were optimized at a range of 55–60 μL/min for the peptide, 15–20 μL/min for PBS, and 10 μL/min for cells.

The two ultrashort peptides, IIZK and IZZK, were compared for printability and the ability to support the chondrogenic differentiation of hBM-MSCs. For 3D bioprinting, three solutions were prepared—peptide solution (13 mg/mL), 7× PBS, and cells in 1× PBS. Each solution was dispensed into an individual inlet of the coaxial nozzle through the microfluidic pumps. Immediately before printing, the selected peptide was dissolved in MilliQ water and loaded in Pump 1. A solution of 7× PBS was loaded in Pump 2. A solution of 1× PBS was loaded in Pump 3. Flow rates of the microfluidic pumps were optimized at a range of 55–60 μL/min for Pump 1, 15–20 μL/min for Pump 2, and 10 μL/min for Pump 3. The flow rates were adjusted within the optimized range, depending on the viscosity of the peptide being used. The printed structures were designed in SolidWorks®, converted into gcode, and bioprinted. The structures included a filled cube (10 × 10 × 1.5 mm), a hollow cylinder (10 × 10 × 10 mm). Multiple samples were printed for each shape to assess shape fidelity. Print resolution, refinement of details, and heights of the samples were compared. A rubric for fidelity assessment was developed to examine printed constructs. The best quality constructs were expected to have excellent resolution, visibly refined details, a consistent thread of gel without any gaps within layers, and to hold shape with taller structures without sagging due to excess water. Imperfect quality constructs had signs of sagging, clumpy deposits of gel, and low-resolution shapes, and could not define structure details.

2.3.2. Bioprinting of cell-laden constructs

The study was approved by the Institutional Biosafety and Ethics Committee (IBEC) at King Abdullah University of Science and Technology (KAUST). Human bone marrow mesenchymal stem cells (hBM-MSCs) were expanded in 2D culture, as described before[31]. Briefly, the cells were cultured at a seeding density of 4×10^3 cells/cm^2 in T175 tissue culture flasks. When cultures reached 70%–80% confluence, the cells were subcultured using 0.25% trypsin. The cells were cultured and maintained in complete growth media, consisting of α-modified minimum essential medium (α-MEM) supplemented with 10% mesenchymal stem cell-qualified fetal bovine serum (FBS), 2 mM L-glutamine, and 1% penicillin/streptomycin (GIBCO, Thermo Fisher, USA). Cells at passages 4–8 were used in printing experiments. For bioprinting, hBM-MSCs were mixed with PBS at a final concentration of 8×10^6 cells/mL and loaded into the microfluidic pumps of the robotic arm bioprinter. In the printing process, the flow rates were 10 μL/min, 55 μL/min, and 8 μL/min for cells, peptide solution, and 5× PBS, respectively. Different cell-laden structures were printed, including cuboids with 10-mm edges and 2.6-mm height and cylinders with 10-mm diameter and 10-mm height. After printing, the printed cell-laden constructs were placed in the CO_2 incubator for 5 min before the addition of complete growth media. The printed cell-laden constructs were placed in standard conditions (37°C, 5% CO_2, and 95% relative humidity), and the media were changed every 3 days.

2.4. Assessment of cell-laden constructs

2.4.1. Cell viability

The viability of 3D-bioprinted cells was assessed using the LIVE/DEAD Viability/Cytotoxicity Kit (Thermo Fisher, USA), in which calcein acetoxymethyl ester (Calcein-AM) is used to detect viable cells, and ethidium homodimer-I (EthD-I) is used to detect dead cells. Cell-laden 3D-bioprinted constructs were washed twice with Dulbecco's phosphate-buffered saline (D-PBS). Then, a staining solution of 2 μM of Calcein-AM and 4 μM of EthD-1 was added to the 3D cell-laden bioprinted constructs and incubated for 45 min in the CO_2 incubator. After incubation, the staining solution was removed, and the 3D-bioprinted constructs were washed with 1× D-PBS. Stained printed cell-laden constructs were imaged using an inverted laser scanning confocal microscope (Zeiss LSM 880 Inverted Confocal Microscope, Germany). Viability percentage was calculated using ImageJ software.

2.4.2. Cytoskeletal staining

The cells were first fixed with 4% formaldehyde solution for 30 min and incubated in a cold cytoskeleton buffer (3 mM $MgCl_2$, 300 mM sucrose and 0.5% Triton X-100 in PBS) for 5 min to permeabilize the cell membranes. The permeabilized cells were incubated in blocking buffer solution (5% FBS, 0.1% Tween-20, and 0.02% sodium azide in PBS) for 30 min at 37°C. For F-actin, anti-mouse IgG (whole molecule)-FITC and rhodamine-phalloidin (1:300) was added to the cells for 1 h. Further, the cells were incubated in DAPI for 5 min to counterstain the nucleus. These fluorescent dye-treated cells were observed and imaged using a laser scanning confocal microscope (Zeiss LSM 710 Inverted Confocal Microscope, Germany).

2.5. Chondrogenic differentiation

Printed cell-laden constructs were placed in the CO_2 incubator for 3 days with complete growth media (α-MEM+ supplements). After 3 days, the constructs were washed three times with 1× PBS for 5 min each, and chondrogenic media were added for 30 days with media exchange every 3 days. The chondrogenic media is composed of DMEM High Glucose (Invitrogen, Thermo Fisher, USA) supplemented with 1% ITS+ premix (Corning, USA), 10^{-7} M dexamethasone (Sigma-Aldrich, Germany), 200 μM ascorbate2-phosphate (Sigma-Aldrich, Germany), 10ng/mL TGF-β3 (R&D systems, USA), 40 μg/mL L-proline (Sigma-Aldrich, Germany), and 1 mM sodium pyruvate and 1% penicillin/streptomycin (Invitrogen, Thermo Fisher, USA).

2.6. Gene expression assessment (quantitative gene expression analysis by RT-PCR)

Total RNA was extracted from the 3D-bioprinted constructs at each specific time point using the mixed isolation procedure using Trizol and Qiagen® RNeasy Mini kit (Qiagen, USA). Total RNA concentration and purity were measured using the NanoDrop 2000 spectrophotometer system (Thermo Fisher Scientific, USA). RNA was reverse-transcribed into cDNA using the SuperScript™ VILO™ cDNA synthesis according to the manufacturer's instructions (Thermo Fisher Scientific, USA). Quantitative polymerase chain reaction (PCR) was performed using TaqMan gene expression assay (Table 1) and TaqMan™ Fast Advanced master mix (Thermo Fisher Scientific, USA) using the Quantstudio 3 system (Thermo Fisher Scientific, USA). The thermal cycling parameters were 50°C for 2 min, then 95°C for 2 min, followed by 40 cycles of 95°C for 1 s and 60°C for 20 s. *GAPDH* gene was used as an endogenous control. Results are displayed as mean ± standard deviation.

2.7. Statistical analysis

All experimental approaches were executed in triplicates. Results are represented as mean ± standard deviation, $n \geq 3$. Statistical analysis was performed using two-way analysis of variance (ANOVA), and values with $p < 0.05$ were considered statistically significant.

Table 1. TaqMan probes

Gene	Catalog number of TaqMan probe	Catalog number
Collagen I (*Col-I*)	Hs00164004_m1	4331182
Collagen II (*Col-II*)	Hs00264051_m1	4331182
Collagen X (*Col-X*)	Hs00166657_m1	4331182
Aggrecan	Hs00202971_m1	4331182
GAPDH	Hs99999905_m1	4448490
Sox9	Hs00165814_m1	4331182

3. Results and discussion

3.1. Ultrashort peptide gelation and characterization

Self-assembling peptide hydrogels have gained significant attention as cell-laden scaffolds due to their biocompatibility, mechanical tunability, and reproducibility. These non–animal-derived materials can form hydrogels through noncovalent interactions (e.g., hydrogen bonding, hydrophobic interaction, etc.). Compared to irreversible covalently crosslinked hydrogels, peptide hydrogels provide a dynamic mechanical microenvironment that can promote better cell growth and spreading[32,33]. However, these physical interactions between peptide molecules generally contribute to the relatively poor mechanical properties, limiting their further use in some emerging biomedical applications, such as bioprinting[34-36]. Therefore, other mechanical integrity and gelation rate improvements while preserving the noncovalent interactions will be a good strategy for developing a superior peptide bioink.

In our previous study, we developed amphiphilic tetrapeptides that can self-assemble to form hydrogel at a relatively low concentration (1 mg/mL) under physiological conditions (Figure 1A)[37]. These ultrashort peptides were mainly composed of a nonpolar hydrophobic tail and positively charged head group. The positively charged residue played an important role in solubility and cell adhesion. Interestingly, two of these ultrashort peptides that displayed faster aggregation kinetic and lower critical gelation concentration contained a highly hydrophobic cyclohexylalanine (Cha) in the middle of their sequences. Through molecular dynamics simulations, the role of Cha residue in the self-assembly of these ultrashort peptides was found to be related to the formation of Cha–Cha cross interaction that can stabilize the β-sheet conformation of the ultrashort peptides[38]. Based on these results, we used

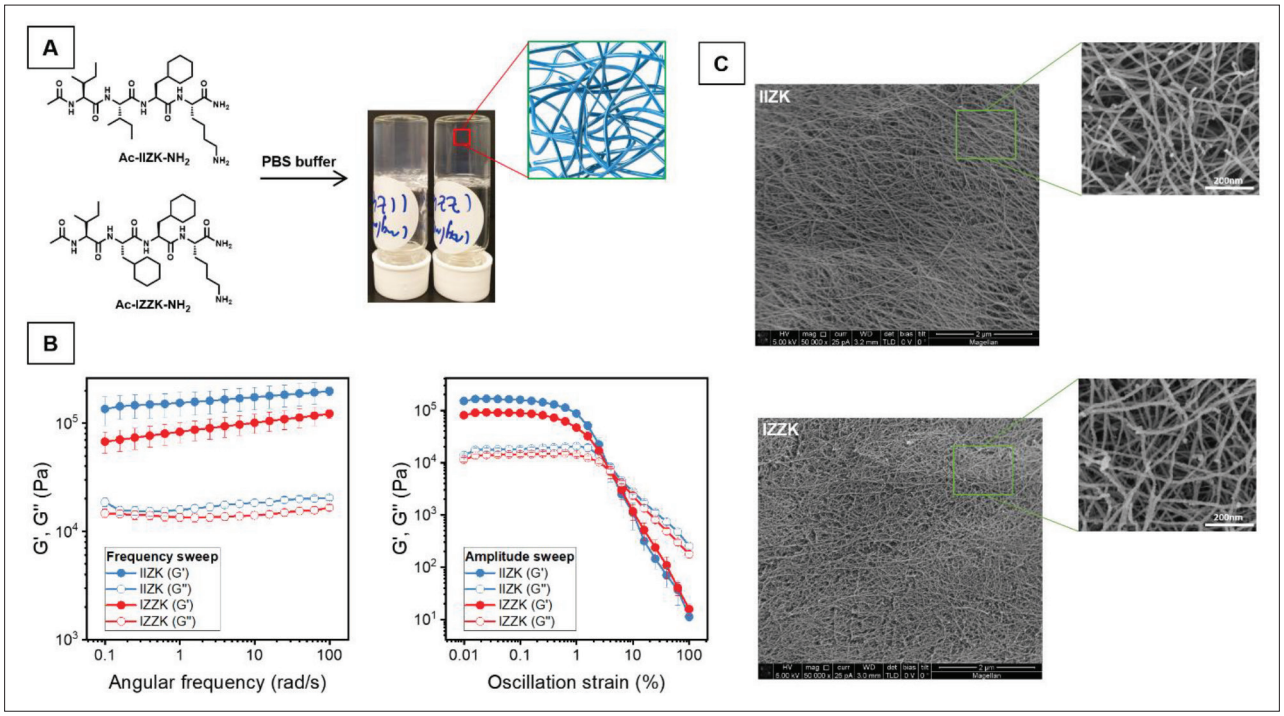

Figure 1. Cyclohexyl alanine-based self-assembling ultrashort peptide hydrogels. (A) IIZK and IZZK peptides start to self-assemble to form hydrogels at relatively low concentration of 1 mg/mL in 1× PBS. (B) Mechanical characterization of ultrashort peptide hydrogels using oscillatory shear measurement. The gels were prepared based on the flow rate ratio of peptide solution and PBS from the printing parameter. (C) SEM micrographs of printed IIZK and IZZK hydrogels.

these two promising ultrashort peptides, IIZK and IZZK, as bioinks for cartilage development *in vivo*.

The mechanical properties of these cyclohexyl alanine-based peptide hydrogels were characterized using oscillatory rheological measurement (Figure 1B). To mimic the same condition as the printed ultrashort peptide bioink, the gel samples were prepared by mixing peptide solution and PBS in two to one ratio. Frequency sweep experiments were performed by applying angular frequency from 100 to 0.1 rad/s at 0.1% strain. The results show an almost linear profile of both ultrashort peptides' storage moduli (G′) and loss moduli (G″), suggesting that both have frequency-independent behavior. This property is also commonly observed in other types of hydrogels[39]. The stiffness of both ultrashort peptides was then determined by the storage modulus at 0.1% strain and 1 rad/s angular frequency. The stiffness of IIZK hydrogel was found to be around 149.06 kPa, which was nearly double of IZZK hydrogel (82.38 kPa). From the amplitude sweep measurement, we observed almost similar deformation behavior between two hydrogels based on their linear viscoelastic (LVE) region. The nanostructure morphology of the ultrashort peptide hydrogels was characterized using a SEM (Figure 1C). The SEM images of both ultrashort peptide gels showed the formation of a porous nanofiber network similar to the extracellular matrix[40].

3.2. Printability and shape fidelity assessment

3D bioprinting experiments were conducted with IIZK and IZZK peptides to assess printability and shape fidelity. A fidelity assessment rubric was developed to quantify observations. Table 1 displays the rubric with a score of 1–5 awarded to each printed construct, depending on performance in terms of gelation, consistency, thread continuity, print resolution, and shape fidelity (Table 2). Several constructs were printed with IZZK and were observed to have quick gelation and maintain thread consistency and continuity (Figure 2A). In terms of print resolution and fidelity, the constructs have sharp resolution with solid walls, indicating strong mechanical stability. Hence, a score of 5 was awarded to IZZK constructs. The hollow cylinder was printed with 54 layers without observing any gaps or clogs during printing. Likewise, several samples of IIZK were printed and observed (Figure 2B). While the peptide powder took slightly longer to dissolve and achieve gelation, IIZK was able to maintain consistent gelation and thread continuity throughout printing. Structure shape was fabricated with very good print resolution and shape fidelity. However, when constructing the hollow cylinder, it was observed

Table 2. Shape fidelity assessment score after 3D bioprinting

Score	Description
1	• Extremely poor resolution • Slow gelation • Forms clumps • Does not form consistent thread of hydrogel • Cannot identify details of structure
2	• Poor resolution • Slow gelation • Clumpy and inconsistent • Structure details are visible but blurry • Begins to fall apart as structure gets taller
3	• Good resolution • Gelation time is reasonable • Forms a consistent thread of hydrogel with occasional clumping • Details of structure are clearly visible but weak • Difficult to hold shape for taller structures
4	• Very good resolution • Gel forms immediately • Consistent thread of hydrogel • Details of structure are cleary visible • Holds shape for tall structures but may have gap in layers due to excess water
5	• Excellent resolution • Gel forms immediately • Consistent thread of hydrogel is very fine • Sharp details are clearly visible • Holds shape for tall structures without sagging due to excess water

that the brief delay in gelation resulted in slightly weaker walls as compared to IZZK which resulted in a score of 4 for IIZK. This was expected as it reflected the difference in stiffness and elasticity in both ultrashort peptides, as seen in rheology readings. Overall, IZZK and IIZK both achieved printability and maintained strong shape fidelity.

3.3. Assessment of 3D-bioprinted cell-laden constructs

Long-term cell viability postprinting is one of the most crucial parameters in evaluating the potential use of bioink for tissue engineering. We had previously demonstrated the high cell viability rate upon 3D bioprinting using peptide-based bioink and the in-house developed robotic arm bioprinting[29], which was further confirmed in this study. The cell viability of 3D-bioprinted cell-laden constructs was assessed using the LIVE/DEAD cell imaging assay. A high percentage of viable cells was observed for both ultrashort peptide bioink (Figure 3A). Using the ultrashort peptide bioinks, instant gelation was achieved without needing harmful crosslinking reagents.

We also investigated the 3D distribution of cells within both ultrashort peptides after bioprinting (Figure 3B). In this regard, hBM-MSCs were 3D-bioprinted using IZZK and IIZK peptides, and then the cell-laden constructs were stained for cytoskeleton, and z-stack 3D images were taken using confocal microscopy. The distribution and arrangement of cells were evaluated within cuboids with 1.0 cm edges and 0.26 cm height. After 21 days of culture, cells in both ultrashort peptides' cell-laden constructs retained their fibroblast-like morphology, with actin fibers well-defined. This cell elongation demonstrates the connection between cells and the ultrashort peptide hydrogel, pointing to the high cytocompatibility of the ultrashort peptide biomaterial and a high level of interaction with the ultrashort peptide hydrogel.

Z-stack images and (x, y, z) projected area images demonstrated the 3D distribution of the cells throughout the printed structures. Using both ultrashort peptide bioink, the cells were found to be dispersed throughout the entire printed constructs with cytoplasmic extensions and cell–cell interaction. A summary comparing the two ultrashort peptide bioink in terms of mechanical properties, printability, shape fidelity, and biocompatibility is listed in Table 3.

3.4. Ultrashort peptide bioink supports chondrogenic differentiation of hMSCs

The differentiation of MSCs is governed by their surrounding microenvironment, including growth stimulation, activation of intracellular signaling, and interaction of cells with the ECM. Besides stimuli of the growth factors, it has been shown that matrix stiffness can regulate and guide the differentiation of these cells toward a specific lineage. For instance, soft substrates were found to promote the differentiation of MSCs toward adipogenic lineage, whereas stiff substrates were found to promote the differentiation toward osteogenic lineage[41,42]. MSCs sense the mechanical signals and biophysical cues from the surrounding ECM, eliciting intracellular signaling pathways that influence and guide cell fate decisions[43,44]. Accordingly, mechanical stiffness is an essential factor for consideration when designing material for tissue engineering applications.

For the first time, we investigated at the molecular level which ultrashort peptide hydrogel (IIZK or IZZK) is better suited for the chondrogenic differentiation of MSCs and can be preferably used in cartilage tissue regenerative medicine applications. Accordingly, to study chondrogenic differentiation, the MSCs were 3D-bioprinted using IIZK or IZZK, and cells were supplemented with chondrogenic induction media. Then, gene expression analysis of cartilage-specific markers using RT-PCR was studied at different time points (days 7 and 14) upon differentiation (Figure 4). Chondrogenic biomarkers such as collagen type II (Col-II), aggrecan, and SRY-related high mobility

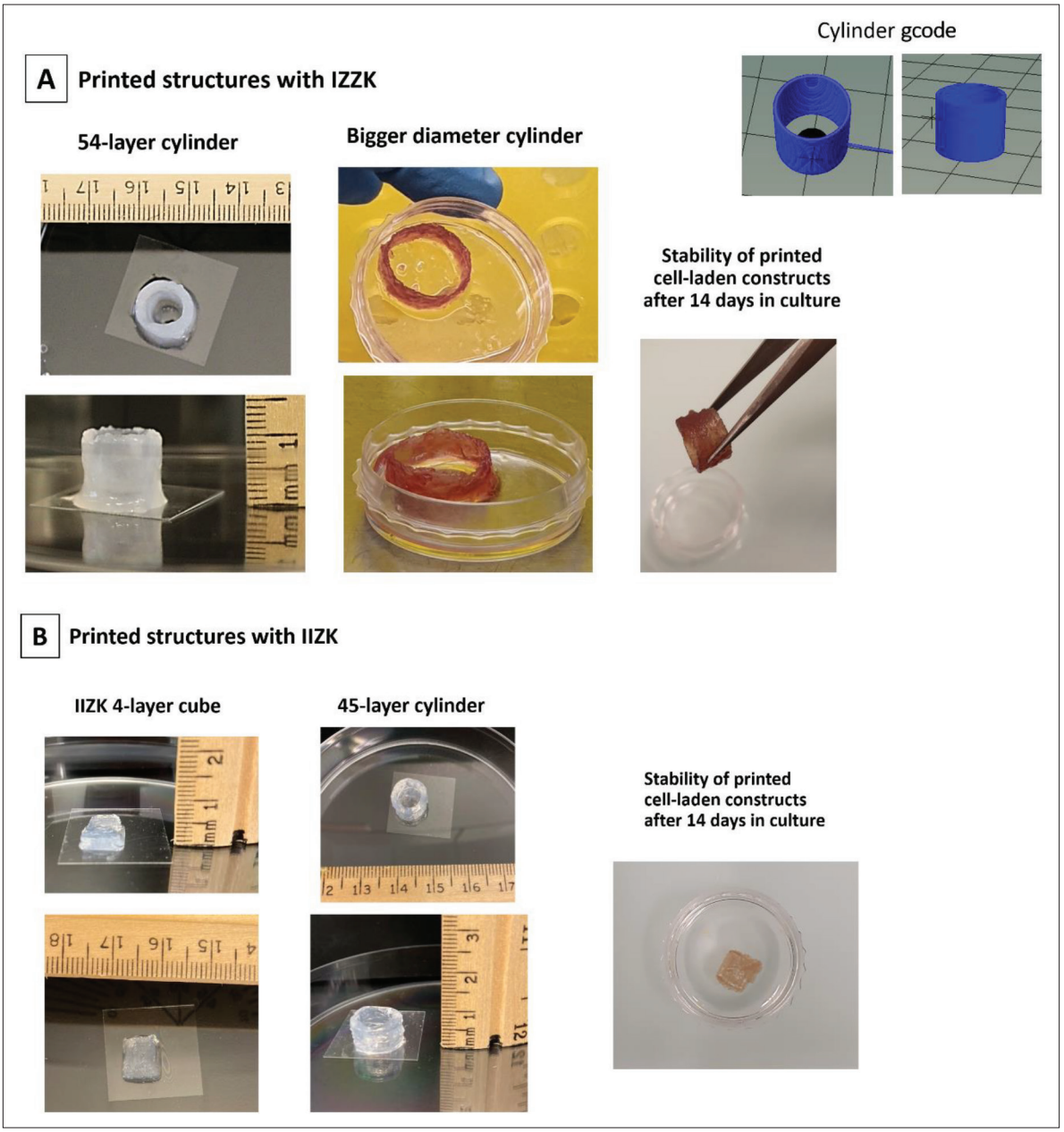

Figure 2. Fidelity and various shape of printed constructs of IIZK and IZZK peptide bioinks.

group-box gene 9 (Sox-9) were evaluated, in addition to collagen type I (Col-I) and collagen type X (Col-X) markers for fibro- and hypertrophic cartilage.

Sox-9 is a master transcription factor in the chondrogenic differentiation of MSCs, controlling the expression of crucial genes involved in chondrogenesis and responsible for Col-II synthesis[45]. At day 7 of differentiation, around a twofold increase in the expression level of Sox-9 was observed on both ultrashort peptides (Figure 4A). Moreover, the expression level of Sox-9 was increased over days in culture, and at day 14, a highly significant difference was observed in MSCs cultured in IZZK peptide compared to IIZK peptide. Col-II is a marker of hyaline cartilage, and during chondrogenesis, it promotes the formation of the ECM[46]. The expression level of Col-II was increased in MSCs on both ultrashort peptide hydrogels (Figure 4A). Interestingly, a high increase in the expression level at day 14 of differentiation, reaching up to 300-fold change, was observed on both ultrashort peptides (Figure 4A). This high increase in the expression of Col-II was among the highest reported[47,48],

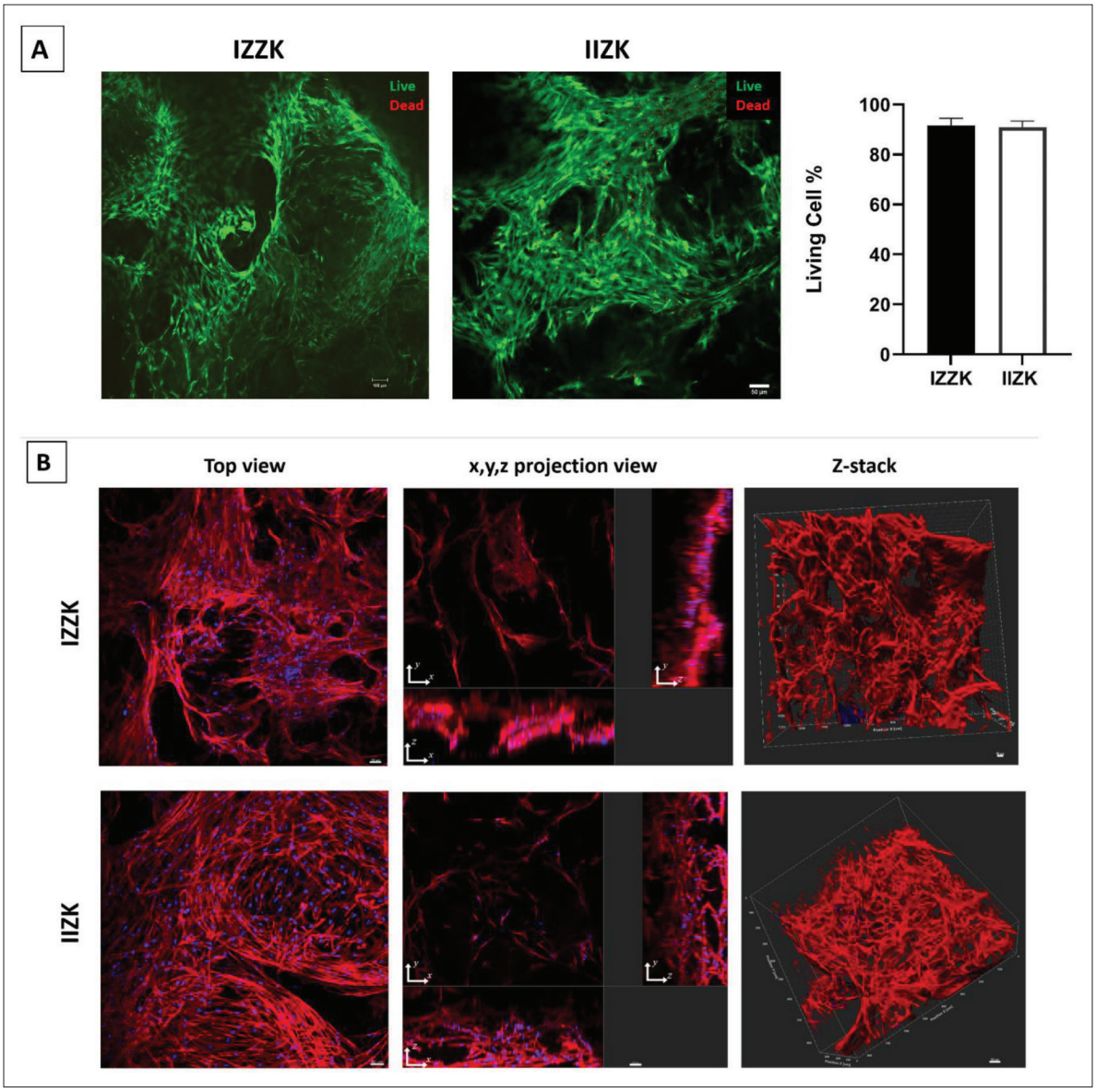

Figure 3. Biocompatibility assessment after 3D bioprinting of IZZK and IIZK peptide. (A) Live/dead long-term cell viability assessment using IZZK and IIZK peptide bioinks (cell viability after 24 days postprinting). Cells were stained with Calcein-AM (green, live cells) and ethidium homodimer-1 (red, dead cells). (B) Cytoskeleton staining to detect morphology and 3D distribution of cells within printed constructs. F-actin was stained with phalloidin (red) and the nucleus with DAPI (blue).

indicating the high potential of the ultrashort peptide bioinks to be used in chondrogenic regenerative medicine applications. No significant difference was observed in the expression level of Coll-II between IZZK and IIZK peptides. In addition, we have studied the expression level of aggrecan, a proteoglycan that forms an essential part of cartilage ECM, giving cartilage tissue the ability to withstand compressive loads[49]. MSCs from both ultrashort peptide bioinks demonstrated an elevated level of aggrecan expression compared to the control on days 7 and 14 (Figure 4A). Notably, at day 14, aggrecan expression was found to be increased approximately 18-fold in IZZK peptide, with a highly significant difference compared to IIZK peptide.

Furthermore, we also aimed to investigate whether our ultrashort peptide bioink supported hyaline cartilage formation over fibro- or hypertrophic cartilage (Figure 4A and B). In this regard, we assessed the Col-II/Col-I and Col-II/Col-X ratios. Although the expression level of fibrocartilage marker Col-I was increased with both ultrashort peptide bioink compared to control at day 7,

Table 3. Characteristic comparison of IZZK and IIZK ultrashort peptide bioinks

	IZZK peptide bioink	IIZK peptide bioink
Stiffness (kPa) after 3D bioprinting	82.38	149.06
Biocompatibility (cell viability)	High viability (92%) at day 24 postprinting	High viability (91%) at day 24 postprinting
Printability and shape fidelity assessment score	5 (excellent resolution), 54-layer cylinder	4 (very good resolution), 45-layer cylinder
Printed structure stability	Constructs were stable for at least 24 days	Constructs were stable for at least 24 days

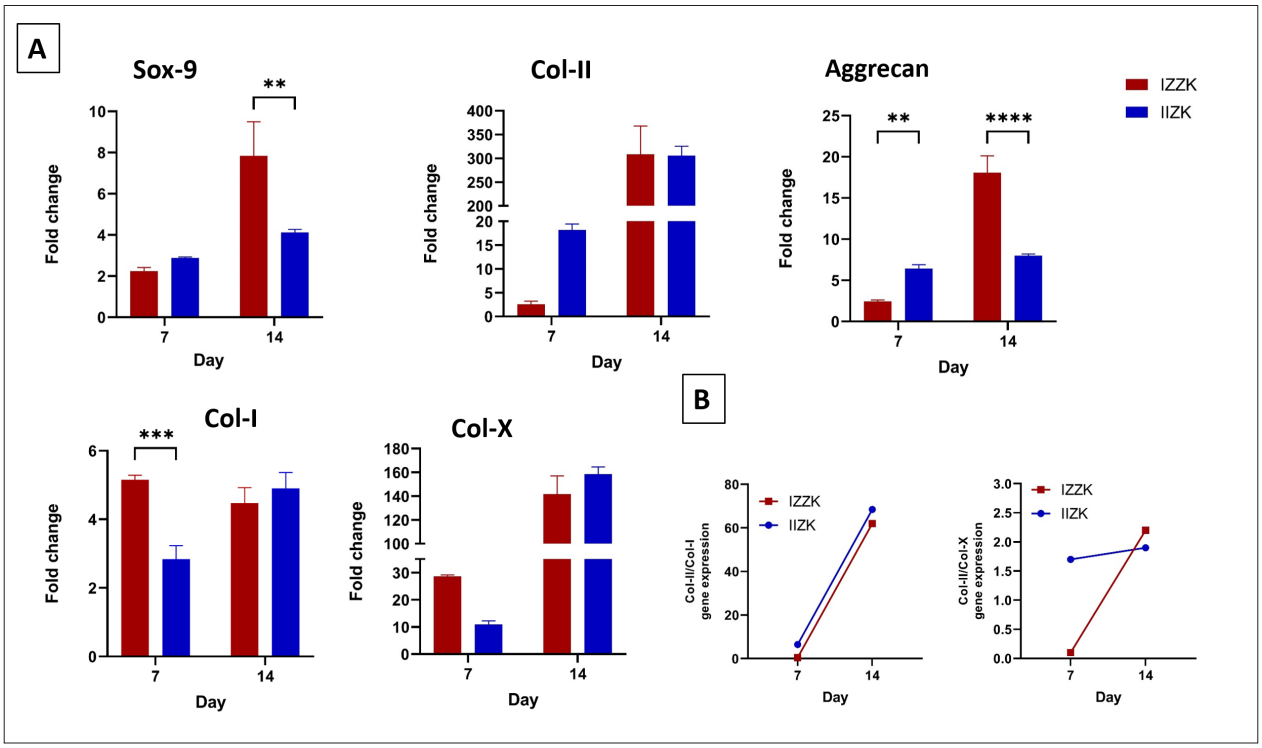

Figure 4. (A) The relative fold change of Sox-9, Col-II, Aggrecan, Col-I, and Col-X during in vitro chondrogenic differentiation was measured by RT-qPCR analysis. $^{**}p < 0.005$, $^{***}p < 0.0001$. (B) Col-II/Col-I and Col-II/Col-X ratios calculated based on relative fold change.

its level stayed the same at day 14 with no significant upregulation (Figure 4A). Importantly, Col-II/Col-I ratio was around 68 and 62 times higher with IZZK and IIZK peptide bioinks, respectively (Figure 4B). On the other hand, at day 14, both ultrashort peptides showed a significant increase in Col-X expression levels compared to the control (Figure 4A). However, the Col-II/Col-X ratio was around two times higher in IZZK and IIZK peptides, respectively (Figure 4B). These results demonstrated that both ultrashort peptides fostered the differentiation of MSCs into chondrocytes with hyaline phenotype and hyaline cartilage formation.

Taken together, the expression profile of Coll-II, Sox-9, and aggrecan suggest that the IZZK peptide is more suitable for cartilage tissue engineering applications. However, considering the ratio of hyaline cartilage marker expression (Col-II) compared to fibro- and hypertrophic cartilage markers (Col-I and Col-X), IIZK peptide holds potential. This could be envisioned by using the two ultrashort peptide bioinks to 3D-bioprint cartilage tissue mimics with different cartilaginous zones, i.e., hyaline cartilage zone and hypertrophic (calcified) cartilage zone. Such a combination is important, as calcified cartilage is essential for engineered tissue integration and function[50].

We observed differences in the mechanical stiffness of printed versus manually formed 3D constructs. Upon manual casting, the stiffness of the IZZK peptide hydrogel was found to be higher than that of the IIZK peptide[29]. Interestingly, we found that the stiffness of the printed IZZK peptide (82 kPa) hydrogel constructs was lower than that of the printed IIZK hydrogel constructs (149kPa) by nearly half a magnitude. This finding has a significant implication for deciding the material and

considering the mechanical properties after bioprinting for tissue engineering. However, to better understand the effect of matrix stiffness on the differentiation of stem cells, microrheology could be studied. In addition, investigating the expression level of osteogenesis- and adipogenesis-associated genes in undifferentiated constructs after 3D bioprinting would provide a better understanding of the matrix stiffness effect on the differentiation of stem cells.

We found that the ultrashort peptide bioink with softer mechanical properties (stiffness) could better support chondrogenesis. Other studies reported similar findings of better chondrogenic differentiation of MSCs on lower-stiffness substrates (soft substrates)[51-54].

4. Conclusions

3D bioprinting is an emerging technology with great potential in regenerative medicine applications, including fabricating tissue mimics and disease models. However, identifying bioinks with high biocompatibility and tailored mechanical stiffness is critical. Mechanical stiffness is essential in guiding stem cell differentiation toward specific lineages. This can be exploited to develop 3D constructs that can direct the differentiation toward the tissue of interest. Here, we reported on two ultrashort peptide bioinks with high biocompatibility and different mechanical stiffness. The uniqueness of those ultrashort peptides stems from being chemically well-defined, thus avoiding any batch-to-batch variations. In addition to their instant gelation at physiological conditions without needing harmful crosslinking reagents, those properties make them great candidates for various tissue engineering applications. We demonstrated that both ultrashort peptides supported the chondrogenic differentiation of human bone marrow MSCs and could be used for cartilage tissue engineering applications. Chondrogenic-specific markers such as Col-II and aggrecan were highly expressed in both ultrashort peptides, demonstrating the potential of those ultrashort peptides in supporting the differentiation of MSCs.

Moreover, due to the differences in the mechanical properties of the IZZK and IIZK peptides, a combination of both ultrashort peptide bioinks could be used in the bioprinting procedure to develop cartilage tissues with different cartilaginous zones.

Acknowledgments

The authors acknowledge Professor Abdalla Awidi from the University of Jordan for providing primary human mesenchymal stem cells.

Funding

This work was financially supported by the King Abdullah University of Science and Technology (KAUST) (grant no: BAS/1/1075-01-01).

Conflict of interest

The authors declare no conflict of interests.

Author contributions

Conceptualization: Charlotte A. E. Hauser, Dana M. Alhattab
Formal analysis: Dana M. Alhattab, Zainab Khan
Investigation: Dana M. Alhattab, Zainab Khan, Hepi H. Susapto
Methodology: Dana M. Alhattab, Zainab Khan, Hepi H. Susapto, Salwa Alshehri
Supervision: Charlotte A. E. Hauser
Writing – original draft: All authors
Writing – review & editing: All authors

All authors have given approval for the final version of the manuscript.

Ethics approval and consent to participate

The study was approved by the Institutional Biosafety and Ethics Committee (IBEC) at King Abdullah University of Science and Technology (KAUST) (21IBEC023).

Consent for publication

Not applicable.

Availability of data

All data are available in the manuscript, and from the corresponding author upon request..

References

1. Seliktar D, 2012, Designing cell-compatible hydrogels for biomedical applications. *Science*, 336(6085):1124–1128.
2. Fang Y, Eglen RM, 2017, Three-dimensional cell cultures in drug discovery and development. *SLAS Discov*, 22(5):456–472.
3. Zhao W, Jin X, Cong Y, *et al.*, 2013, Degradable natural polymer hydrogels for articular cartilage tissue engineering. *J Chem Technol Biotechnol*, 88(3):327–339.
4. Lu B, Yuk H, Lin S, *et al.*, 2019, Pure pedot: Pss hydrogels. *Nat Commun*, 10(1):1043.
5. Yang J, Bai R, Suo Z, 2018, Topological adhesion of wet materials. *Adv Mater*, 30(25):1800671.
6. Seow WY, Hauser CA, 2014, Short to ultrashort peptide hydrogels for biomedical uses. *Mater Today*, 17(8):381–388.

7. Richardson SM, Kalamegam G, Pushparaj PN, *et al.*, 2016, Mesenchymal stem cells in regenerative medicine: Focus on articular cartilage and intervertebral disc regeneration. *Methods*, 99:69–80.
8. Somoza RA, Welter JF, Correa D, *et al.*, 2014, Chondrogenic differentiation of mesenchymal stem cells: Challenges and unfulfilled expectations. *Tissue Eng Part B: Rev*, 20(6):596–608.
9. Ng WL, Chua CK, Shen Y-F, 2019, Print me an organ! Why we are not there yet. *Progr Polym Sci*, 97:101145.
10. Huang J, Xiong J, Wang D, *et al.*, 2021, 3D bioprinting of hydrogels for cartilage tissue engineering. *Gels*, 7(3):144.
11. Han X, Chang S, Zhang M, 2021, Advances of hydrogel-based bioprinting for cartilage tissue engineering. *Front Bioeng Biotechnol*, (9):816–829.
12. Huang J, Huang Z, Liang Y, *et al.*, 2021, 3D printed gelatin/hydroxyapatite scaffolds for stem cell chondrogenic differentiation and articular cartilage repair. *Biomater Sci*, 9(7):2620–2630.
13. Xiongfa J, Hao Z, Liming Z, *et al.*, 2018, Recent advances in 3D bioprinting for the regeneration of functional cartilage. *Regen Med*, 13(1):73–87.
14. Ng WL, Lee JM, Zhou M, *et al.*, 2020, Vat polymerization-based bioprinting—Process, materials, applications and regulatory challenges. *Biofabrication*, 12(2):022001.
15. Jiang T, Munguia-Lopez JG, Flores-Torres S, *et al.*, 2019, Extrusion bioprinting of soft materials: An emerging technique for biological model fabrication. *Appl Phys Rev*, 6(1):011310.
16. Li X, Liu B, Pei B, *et al.*, 2020, Inkjet bioprinting of biomaterials. *Chem Rev*, 120(19):10793–10833.
17. Tekin E, Smith PJ, Schubert US, 2008, Inkjet printing as a deposition and patterning tool for polymers and inorganic particles. *Soft Matter*, 4(4):703–713.
18. Villar G, Graham AD, Bayley H, 2013, A tissue-like printed material. *Science*, 340(6128):48–52.
19. Xu T, Jin J, Gregory C, *et al.*, 2005, Inkjet printing of viable mammalian cells. *Biomaterials*, 26(1):93–99.
20. Ng WL, Huang X, Shkolnikov V, *et al.*, 2022, Controlling droplet impact velocity and droplet volume: Key factors to achieving high cell viability in sub-nanoliter droplet-based bioprinting. *Int J Bioprint*, 8(1): 424–440.
21. Zhang LG, Leong K, Fisher JP, 2022, *3D Bioprinting and Nanotechnology in Tissue Engineering and Regenerative Medicine*, Academic Press.
22. Xue K, Zhang X, Gao Z, *et al.*, 2019, Cartilage progenitor cells combined with PHBV in cartilage tissue engineering. *J Transl Med*, 17(1):1–11.
23. Weissenberger M, Weissenberger MH, Wagenbrenner M, *et al.*, 2020, Different types of cartilage neotissue fabricated from collagen hydrogels and mesenchymal stromal cells via SOX9, TGFB1 or BMP2 gene transfer. *PLoS One*, 15(8):e0237479.
24. Ibrahim MI, Alsafadi D, Alamry KA, *et al.*, 2021, Properties and applications of poly(3-hydroxybutyrate-co-3-hydroxyvalerate) biocomposites. *J Polym Environ*, 29:1010–1030.
25. Montalbano G, Borciani G, Pontremoli C, *et al.*, 2019, Development and biocompatibility of collagen-based composites enriched with nanoparticles of strontium containing mesoporous glass. *Materials*, 12(22):3719.
26. Khan Z, Kahin K, Rauf S, *et al.*, 2019, Optimization of a 3D bioprinting process using ultrashort peptide bioinks. *Int J Bioprint*, 5(1):173.
27. Di Bella C, Fosang A, Donati DM, *et al.*, 2015, 3D bioprinting of cartilage for orthopedic surgeons: Reading between the lines. *Front Surg*, 2:39.
28. Wei W, Ma Y, Yao X, *et al.*, 2021, Advanced hydrogels for the repair of cartilage defects and regeneration. *Bioact Mater*, 6(4):998–1011.
29. Susapto HH, Alhattab D, Abdelrahman S, *et al.*, 2021, Ultrashort peptide bioinks support automated printing of large-scale constructs assuring long-term survival of printed tissue constructs. *Nano Lett*, 21(7):2719–2729.
30. Kahin K, Khan Z, Albagami M, *et al.*, 2019, Development of a robotic 3D bioprinting and microfluidic pumping system for tissue and organ engineering. *Microfluidics, BioMEMS, and Medical Microsystems XVII*, SPIE, 130–139.
31. Alhattab D, Jamali F, Ali D, *et al.*, 2019, An insight into the whole transcriptome profile of four tissue-specific human mesenchymal stem cells. *Regen Med*, 14(9):841–865.
32. Rajbhandary A, Nilsson BL, 2016, Self-assembling hydrogels, *In Gels Handbook: Fundamentals, Properties and Application; Volume 1: Fundamentals of Hydrogels*, New Jersey, 219–250.
33. Wang X, Horii A, Zhang S, 2008, Designer functionalized self-assembling peptide nanofiber scaffolds for growth, migration, and tubulogenesis of human umbilical vein endothelial cells. *Soft Matter*, 4(12):2388–2395.
34. Memic A, Alhadrami HA, Hussain MA, *et al.*, 2016, Hydrogels 2.0: Improved properties with nanomaterial composites for biomedical applications. *Biomed Mater*, 11(1):014104.
35. Huang L-C, Wang H-C, Chen L-H, *et al.*, 2019, Bioinspired self-assembling peptide hydrogel with proteoglycan-assisted growth factor delivery for therapeutic angiogenesis. *Theranostics*, 9(23):7072–7087.
36. Unagolla JM, Jayasuriya AC, 2020, Hydrogel-based 3D bioprinting: A comprehensive review on cell-laden hydrogels, bioink formulations, and future perspectives. *Appl Mater Today*, 18:100479.
37. Susapto HH, Alhattab D, Abdelrahman S, *et al.*, 2021, Ultrashort peptide bioinks support automated printing of large-scale constructs assuring long-term survival of printed tissue constructs. *Nano Lett,* 21(7):2719–2729.

38. Waters ML, Aromatic interactions in peptides: Impact on structure and function. *Pept Sci*, 76(5):435–445.

39. Greenfield MA, Hoffman JR, de la Cruz MO, *et al.*, 2010, Tunable mechanics of peptide nanofiber gels. *Langmuir*, 26(5):3641–3647.

40. Loo Y, Lakshmanan A, Ni M, *et al.*, 2015, Peptide bioink: Self-assembling nanofibrous scaffolds for three-dimensional organotypic cultures. *Nano Lett*, 15(10):6919–6925.

41. Wu L, Magaz A, Wang T, *et al.*, 2018, Stiffness memory of indirectly 3D-printed elastomer nanohybrid regulates chondrogenesis and osteogenesis of human mesenchymal stem cells. *Biomaterials*, 186:64–79.

42. El-Rashidy AA, El Moshy S, Radwan IA, *et al.*, 2021, Effect of polymeric matrix stiffness on osteogenic differentiation of mesenchymal stem/progenitor cells: Concise review. *Polymers*, 13(17):2950.

43. Fahy N, Alini M, Stoddart MJ, 2018, Mechanical stimulation of mesenchymal stem cells: Implications for cartilage tissue engineering. *J Orthop Res*, 36(1):52–63.

44. Hao J, Zhang Y, Jing D, *et al.*, 2015, Mechanobiology of mesenchymal stem cells: Perspective into mechanical induction of MSC fate. *Acta Biomater*, 20:1–9.

45. Almalki SG, Agrawal DK, 2016, Key transcription factors in the differentiation of mesenchymal stem cells. *Differentiation*, 92(1–2):41–51.

46. Liu Y, Shah KM, Luo J, 2021, Strategies for articular cartilage repair and regeneration. *Front Bioeng Biotechnol*, 9:1328.

47. Idaszek J, Costantini M, Karlsen TA, *et al.*, 2019, 3D bioprinting of hydrogel constructs with cell and material gradients for the regeneration of full-thickness chondral defect using a microfluidic printing head. *Biofabrication*, 11(4):044101.

48. Costantini M, Idaszek J, Szöke K, *et al.*, 2016, 3D bioprinting of BM-MSCs-loaded ECM biomimetic hydrogels for in vitro neocartilage formation. *Biofabrication*, 8(3):035002.

49. Roughley PJ, Mort JS, 2014, The role of aggrecan in normal and osteoarthritic cartilage. *J Exp Orthop*, 1(1):1–11.

50. Hollenstein J, Terrier A, Cory E, *et al.*, 2015, Mechanical evaluation of a tissue-engineered zone of calcification in a bone–hydrogel osteochondral construct. *Comput Methods Biomech Biomed Eng*, 18(3):332–337.

51. Olivares-Navarrete R, Lee EM, Smith K, *et al.*, Substrate stiffness controls osteoblastic and chondrocytic differentiation of mesenchymal stem cells without exogenous stimuli. *PLoS One*, 12(1):e0170312.

52. Zhou Y, Qiu J, Wan L, *et al.*, 2022, The effect of matrix stiffness on the chondrogenic differentiation of mesenchymal stem cells. *J Mol Histol*, 53(5):805–816.

53. Mohammed M, Lai T-S, Lin H-C, 2021, Substrate stiffness and sequence dependent bioactive peptide hydrogels influence the chondrogenic differentiation of human mesenchymal stem cells. *J Mater Chem B*, 9(6):1676–1685.

54. Park JS, Chu JS, Tsou AD, *et al.*, 2011, The effect of matrix stiffness on the differentiation of mesenchymal stem cells in response to TGF-β. *Biomaterials*, 32(16):3921–3930.